

Slippery diffusion-limited aggregation

Clair R. Seager^{1,*} and Thomas G. Mason^{2,†}¹*Department of Physics and Astronomy, University of California-Los Angeles, Los Angeles, California 90095, USA*²*Department of Physics and Astronomy, Department of Chemistry and Biochemistry, and California NanoSystems Institute, University of California—Los Angeles, Los Angeles, California 90095, USA*

(Received 22 August 2006; published 18 January 2007)

Colloidal particles that interact through strong, short-range, secondary attractions in liquids form irreversible “slippery” bonds that are not shear-rigid. Through event-driven simulations of slippery attractive spheres, we show that space-filling fractal clusters still emerge from the process of “slippery” diffusion-limited aggregation (DLA). Although slippery and classic DLA clusters have the same fractal dimension, $d_f=2.5$, their average coordination numbers are quite different: $\langle z_S \rangle=6$ whereas $\langle z_C \rangle=2$. Local tetrahedral attractive jamming of the particles leads to a structure factor, $S(q)$, that exhibits dense cluster peaks at higher wave numbers, q , and a fractal power-law rise toward lower q .

DOI: [10.1103/PhysRevE.75.011406](https://doi.org/10.1103/PhysRevE.75.011406)

PACS number(s): 61.43.Hv, 61.43.Bn, 82.70.Dd, 05.70.Ln

A large class of beautiful and intricate structures can emerge through nonequilibrium aggregation processes involving attractive particles. For extremely dilute particle volume fractions, ϕ , solid colloids that diffuse through a continuous liquid phase can aggregate with strong shear-rigid bonds to form tenuous fractals through classic diffusion-limited aggregation (DLA) [1,2]. When solid gold particles in solution enter a primary minimum in their pair interaction potential, due to van der Waals attractions, they physically touch, forming a shear-rigid contact [3–5]; the fractal dimension, d_f , of DLA in three-dimensions is 2.49 [2]. At higher ϕ , DLA clusters can aggregate with other neighboring clusters and form percolating gel structures through diffusion-limited cluster aggregation (DLCA) with $d_f \approx 1.9$ [6–9]. In reaction-limited aggregation (RLA), particles can unbind from the cluster with a certain probability and later rejoin the cluster, producing fractal RLA clusters [7,10]. In DLA, RLA, and other forms of nonequilibrium growth, including Eden growth [11,12], thermodynamics cannot describe the structures because the growth depends upon the kinetic history of how particles attach to the cluster.

Shear-rigid bonds are only one important case: two liquid droplets cannot form a shear-rigid bond [13,14]. When a deep, short-range “secondary” minimum, ε , in their pair interaction potential is created, they can become strongly attractive, yet not form shear-rigid bonds [14,15]. Depletion attractions between microspheres induced by polymer or surfactant micelles and also temperature-dependent surface charge condensation effects can also create such short-range secondary attractions [16–19]. If ε is somewhat larger than thermal energy, $k_B T$, a dense liquidlike floc of particles forms. However, if ε is quenched, so $\varepsilon \gg k_B T$, the lubricated particles become linked by irreversible “slippery” bonds, precluding shear-rigidity, and a nonequilibrium structure forms. Slippery bonds do not break, yet they still permit each bound sphere in a pair to rotationally diffuse. Moreover, each

sphere can translationally diffuse over the surface of the other. By contrast, shear-rigid bonding creates a rigid dumbbell, precluding internal dynamics. These differences in bonding, although subtle, can strongly affect nonequilibrium structures.

The impact of slippery bonding has been seen in neutron scattering measurements of the wave-number-dependent structure factor, $S(q)$, of aggregated nanoemulsion droplets. Peaks at high q have been associated with the aggregation of small dense clusters to form a tenuous fractal gel [13]. Concurrent real-space confocal microscopy studies of solid microspheres interacting through depletion attractions have also revealed interconnected gels [20] and a piecewise $S(q)$ with a gap in the crossover between the particle-scale and the fractal gel structures [19]. Both experiments support the conjecture [14] that slippery-bonded spheres form tetrahedra that can serve as rigid building blocks for tenuous and disordered fractal aggregates and gels. Molecular dynamics simulations have begun to address concentrated systems that form through slippery interactions as a function of the well depth [18,21–24], yet the simplest DLA process involving slippery bonds for $\phi \rightarrow 0$ of attractively jammed spheres [25] in three dimensions remains unexplored.

In this paper, we use event-driven simulations to study “slippery” diffusion-limited aggregation (SDLA). Identical spheres of radius, a , are released one at a time and diffuse until they touch a growing cluster. After making contact, each sphere is locked into the cluster using one of three rules: (1) classic DLA (CDLA): the sphere is rigidly attached where it first touches; (2) equilateral DLA (EDLA): the sphere is locked into the node corresponding to the nearest equilateral triangle on the cluster’s surface; and (3) slippery DLA: the sphere is locked into the node formed by the nearest triangle, whether equilateral or not. We show that SDLA and CDLA have essentially the same d_f , yet the mass-distance scaling curve reveals locally dense tetrahedral structures for SDLA. The probability distributions of nearest neighbors yield an average coordination number for SDLA of $\langle z_S \rangle=6.0$, whereas, CDLA has only $\langle z_C \rangle=2.0$. For SDLA, the distribution of edge-lengths of the nonequilateral triangular bases exhibits pronounced peaks corresponding to special

*Present address: Department of Physics, New York University, New York, NY 10003, USA.

†Corresponding author: Email address: mason@chem.ucla.edu

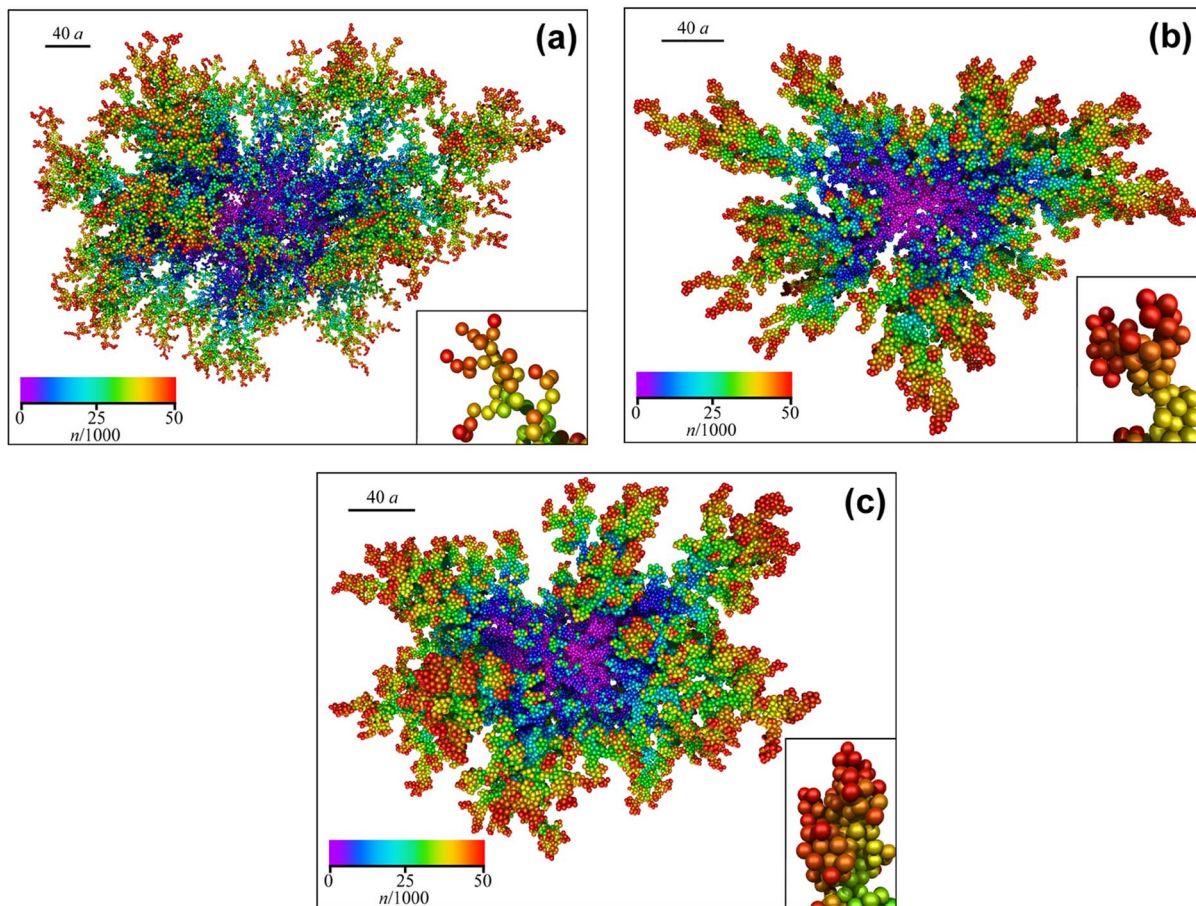


FIG. 1. (Color online) Aggregates ($N=50\,000$ spheres) obtained by (a) CDLA: classic shear-rigid bonding, (b) EDLA: each newly added sphere jams into the nearest node formed by an equilateral triangular face, and (c) SDLA: each newly added sphere jams into a node formed by any triangular face. Insets show detailed views of cluster tips. Scale bars represent 40 sphere radii (at the cluster's center). Colors encode the order of release of the particles, and n refers to the release number.

local packing configurations that are frequently encountered. The calculated structure factor for SDLA shows characteristic features of locally dense particle jamming at high q and fractal scaling toward low q . This predicted $S(qd)$, where $d=2a$, captures many of the essential features found in recent experiments.

CDLA clusters are made using the method of Witten and Sander [1,2]. A “seed” sphere is fixed; additional spheres are released one at a time and perform a random walk. If a diffusing sphere touches the cluster, then it is rigidly bonded to the cluster. Spheres that diffuse too far away from the cluster are discarded and a new sphere is injected. The distance of each newly injected sphere to the cluster is optimized to reduce the diffusion time [2]. A list of nearest neighbors is updated as particles are added to the cluster. CDLA clusters are tenuous fractals and have spindly local structures [Fig. 1(a)].

In EDLA, the first four spheres form an equilateral tetrahedral “seed.” Spheres are injected as for CDLA, yet when a diffusing sphere encounters the growing cluster, nearest-neighbor distances in the cluster are used to determine if a node corresponding to an equilateral triangular face on the surface of the cluster is immediately adjacent to the first-encountered sphere. If so, the diffusing sphere is locked into

that node. If not, the trial is discarded. Thus EDLA clusters are comprised entirely of equilateral tetrahedra. EDLA enforces locally dense jamming of spheres with only one bond angle and provides a first step towards modeling the effects of diffusion of slippery spheres on the cluster's surface. Strikingly, EDLA also creates a fractal cluster [Fig. 1(b)]; EDLA aggregate arms (inset) are dense compared to the spindly structures of CDLA.

Since nonequilateral triangular nodes can also capture spheres, we have created a more realistic algorithm, SDLA, that locks spheres into the nearest viable equilateral and non-equilateral triangular sites on the growing cluster. SDLA effectively models the most probable final location of a newly added sphere after it touches the cluster, diffuses over the cluster's surface, and locks into a nearby node. SDLA clusters [Fig. 1(c)] are fractal yet more compact than either CDLA or EDLA clusters. The event-driven simulation can omit very rare events of bridging of a single sphere captured between two proximate spheres in neighboring arms of the cluster which nearly touch. Such “bridging” spheres never lock into a node and retain some translational freedom that could affect dynamics [26], yet they influence the average static structure very little.

We obtain d_f for CDLA, EDLA, and SDLA clusters by

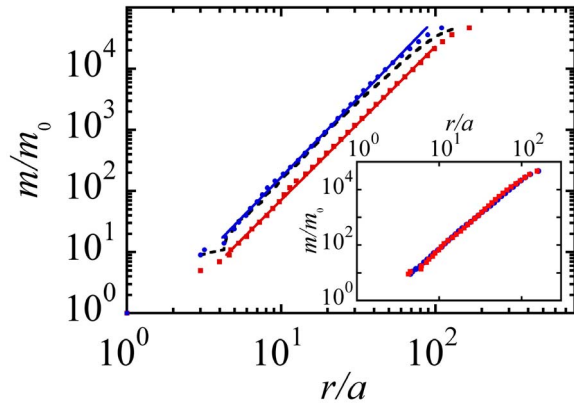


FIG. 2. (Color online) Mass, m , of the fraction of the cluster enclosed within an imaginary sphere of radius, r , which is centered on a starting seed particle: classic DLA (■), equilateral DLA (dashed line), and slippery DLA (●). The axes are normalized by the mass, m_0 , and the radius, a , of a single spherical particle, respectively. The solid lines are fits in the scaling region, yielding $d_f=2.5\pm 0.1$. Inset: classic and slippery DLA scale together when r/a for SDLA is multiplied by 1.5.

plotting the dimensionless mass, m/m_0 , versus dimensionless radius, r/a , in log-log format in Fig. 2. For the smallest r/a , discreteness due to limited statistics is seen, yet for larger r/a , m/m_0 becomes smooth and straight, following $(m/m_0) \sim (r/a)^{d_f}$. Surprisingly, for all three simulation types, we find $d_f=2.5\pm 0.1$. The result for CDLA is consistent with earlier simulations [2]. Although EDLA closely resembles SDLA in the inner regions of the cluster, the equilateral constraint of EDLA creates thinner arms at the extremities; this can be seen by an earlier departure from the power-law scaling for EDLA toward high r/a . For all types of DLA, as r approaches the length of the cluster's longest arm, the fractal scaling regime ends due to the cluster's finite size, and m/m_0 saturates to N .

The scaling behavior of m/m_0 for slippery DLA can be shifted onto the classic DLA result by simply multiplying r/a by a factor of 1.5 [Fig. 2 (inset)]. After rescaling, the overlap is excellent over a wide range of r/a above the limit where discreteness effects are seen. Overall, the factor of 1.5 is consistent with half of the separation between the centers of two interlocked tetrahedra. Such tetrahedra made of four spheres each have four dimpled faces that can rigidly interlock with other tetrahedra through slippery bonds. Since tetrahedra added randomly to a growing cluster do not pack with long range order to fill space, the growing cluster will not be a dense crystal but instead will be a tenuous fractal. In essence, SDLA clusters can be created by taking CDLA clusters and replacing the spheres that form shear rigid bonds with rigidly interlocking tetrahedra.

The probability density distributions, $p_z(z)$, of the local coordination number, z , obtained from the neighbor lists are shown in Fig. 3. For CDLA, p_z peaks at two nearest neighbors, corresponding to rigid chains of spheres, and the average is $\langle z_C \rangle = 2.0$. Branched structures with three neighbors are common, but branches with four or more neighbors are relatively rare. By contrast, for EDLA and SDLA, $p_z=0$ for z

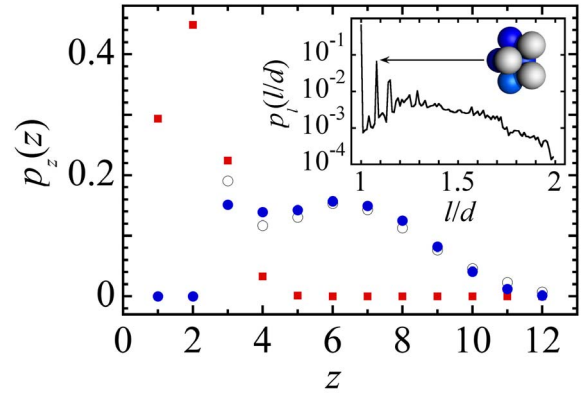


FIG. 3. (Color online) Normalized probability distribution of local coordination number, $p_z(z)$, for CDLA ($\langle z_C \rangle = 2.0$ (■)); EDLA ($\langle z_E \rangle = 6.0$ (○)); and SDLA ($\langle z_S \rangle = 6.0$ (●)). Inset: the distribution of dimensionless edge lengths, $p_l(l/d)$, of triangular bases prior to adding a new sphere for SDLA. The isosceles base triangle (white spheres), has an edge length of 1.08, accounting for the peak (arrow).

< 3 , consistent with rules that demand tetrahedral structures. For EDLA, the relatively high probability at $z=3$ results from the large number of spheres that have recently joined the surface of the cluster. For SDLA p_z resembles EDLA in shape, and the maximum still occurs at $\langle z_S \rangle = 6.0$, yet the surface contribution at $z=3$ is smaller, consistent with compact branch tips. In Fig. 3 (inset), we show the edge length distribution $p_l(l/d)$ of the triangles on the surfaces of SDLA clusters into which incoming spheres are locked. The spikes in this distribution that occur at $l/d=1.08$ and higher values reflect edge lengths of special triangles due to local packing arrangements that are frequently encountered.

The structure factor calculated for SDLA is shown in Fig. 4. The peaks at high qd are more pronounced than for CDLA, since SDLA has a larger $\langle z \rangle$ and a denser local structure, yet no long-range order. As qd decreases from the largest peak, S goes through a minimum and begins to increase

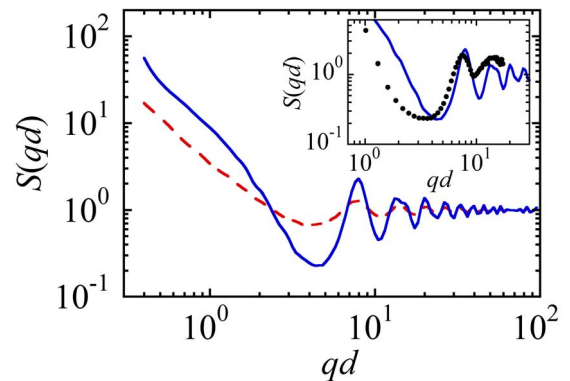


FIG. 4. (Color online) Structure factor, $S(qd)$, vs dimensionless wave number, qd , for aggregates formed by CDLA (dashed line) and SDLA (solid line). Nearest-neighbor peaks at high qd are more pronounced for SDLA. Inset: comparison of $S(qd)$ calculated for SDLA (line) to neutron scattering measurements of slippery nanoemulsion droplets (points).

again, reflecting the scattering from the larger-scale fractal structure. The position and magnitude of the first and second peaks and the magnitude of the minimum at lower qd of the measured $S(qd)$ from neutron scattering of uniform nanoemulsions at $\phi \approx 0.05$ [13] are reasonably well-described by SDLA (inset). The nanoemulsion's S results from a slippery cluster-cluster aggregation process, which is different than SDLA as $\phi \rightarrow 0$, so a deviation toward the lowest qd is expected.

SDLA is an important limiting case of attractive colloidal glasses that can be formed over a larger range of ε and ϕ . It provides a clear particle-scale picture that shows how tenuous fractal clusters can still be formed even when attractive bonds are not shear-rigid. The slippery attractive jamming of spherical particles creates clusters at high z that are comprised of locally dense tetrahedra; the resulting corrugation on the cluster's surface leads to nodes that quickly trap newly added particles and prevent further surface diffusion. As conjectured [14], these local tetrahedra act as larger rescaled anisotropic "particles" that aggregate through shear-rigid bonds to form globally disordered structures with the

same d_f as CDLA. For this reason, observations of fractal structures and gels may be incorrectly interpreted as arising from CDLA rather than SDLA. By analogy, one would expect slippery DLCA (SDLCA) to also have $d_f \approx 1.9$, corresponding to classic DLCA formed with shear-rigid bonds. Indeed, this prediction is in reasonable accord with light scattering measurements yielding $d_f \approx 1.8$ for microscale emulsions [15,27,28].

Slippery DLA opens the door to many exciting future directions. By building many SDLA clusters simultaneously and allowing these clusters to diffuse and connect, it will be possible to create SDLCA structures, including tenuous networks and percolating gels. Introducing polydispersity and nonspherical building blocks will give rise to new and interesting slippery aggregation phenomena. Further statistical analyses of SDLA and SDLCA clusters will provide additional insight into attractively jammed systems.

We thank NSF (CHE-0450022), Dr. McTague, and the California NanoSystems Institute for support, and A. Levine, D. Blair, and R. Bruinsma for discussions.

-
- [1] T. A. Witten and L. M. Sander, *Phys. Rev. Lett.* **47**, 1400 (1981).
- [2] L. M. Sander, *Contemp. Phys.* **41**, 203 (2000).
- [3] D. A. Weitz, J. S. Huang, M. Y. Lin, and J. Sung, *Phys. Rev. Lett.* **54**, 1416 (1985).
- [4] P. Dimon, S. K. Sinha, D. A. Weitz, C. R. Safinya, G. S. Smith, W. A. Varady, and H. M. Lindsay, *Phys. Rev. Lett.* **57**, 595 (1986).
- [5] M. Y. Lin, H. M. Lindsay, D. A. Weitz, R. Klein, R. C. Ball, and P. Meakin, *J. Phys.: Condens. Matter* **2**, 3093 (1990).
- [6] P. Meakin and R. Jullien, *J. Chem. Phys.* **89**, 246 (1988).
- [7] R. Jullien and M. Kolb, *J. Phys. A* **17**, L639 (1984).
- [8] M. Carpineti and M. Giglio, *Phys. Rev. Lett.* **68**, 3327 (1992).
- [9] M. Carpineti and M. Giglio, *Phys. Rev. Lett.* **70**, 3828 (1993).
- [10] R. C. Ball, D. A. Weitz, T. A. Witten, and F. Leyvraz, *Phys. Rev. Lett.* **58**, 274 (1987).
- [11] Z. Racz and M. Plischke, *Phys. Rev. A* **31**, 985 (1985).
- [12] R. L. Smith and S. D. Collins, *Phys. Rev. A* **39**, 5409 (1989).
- [13] J. N. Wilking, S. M. Graves, C. B. Chang, K. Meleson, M. Y. Lin, and T. G. Mason, *Phys. Rev. Lett.* **96**, 015501 (2006).
- [14] T. G. Mason, A. H. Krall, H. Gang, J. Bibette, and D. A. Weitz, in *Encyclopedia of Emulsion Technology*, edited by P. Becher (Marcel Dekker, New York, 1996), Vol. 4, p. 299.
- [15] J. Bibette, T. G. Mason, H. Gang, and D. A. Weitz, *Phys. Rev. Lett.* **69**, 981 (1992).
- [16] W. C. K. Poon, A. D. Pirie, and P. N. Pusey, *Faraday Discuss.* **101**, 65 (1995).
- [17] K. N. Pham, A. M. Puertas, J. Bergenholtz, S. U. Egelhaaf, A. Moussaid, P. N. Pusey, A. B. Schofield, M. E. Cates, M. Fuchs, and W. C. K. Poon, *Science* **296**, 104 (2002).
- [18] M. E. Cates, M. Fuchs, K. Kroy, W. C. K. Poon, and A. M. Puertas, *J. Phys.: Condens. Matter* **16**, S4861 (2004).
- [19] S. Manley, H. M. Wyss, K. Miyazaki, J. C. Conrad, V. Trappe, L. J. Kaufman, D. R. Reichman, and D. A. Weitz, *Phys. Rev. Lett.* **95**, 238302 (2005).
- [20] P. J. Lu, J. C. Conrad, H. M. Wyss, A. B. Schofield, and D. A. Weitz, *Phys. Rev. Lett.* **96**, 028306 (2006).
- [21] A. M. Puertas, M. Fuchs, and M. E. Cates, *Phys. Rev. E* **67**, 031406 (2003).
- [22] J. J. Cerda, T. Sintes, C. M. Sorensen, and A. Chakrabarti, *Phys. Rev. E* **70**, 011405 (2004).
- [23] J. C. Gimel, T. Nicolai, and D. Durand, *J. Sol-Gel Sci. Technol.* **15**, 129 (1999).
- [24] J. C. Gimel, T. Nicolai, and D. Durand, *Phys. Rev. E* **66**, 061405 (2002).
- [25] A. J. Liu and S. R. Nagel, *Nature (London)* **396**, 21 (1998).
- [26] A. H. Krall and D. A. Weitz, *Phys. Rev. Lett.* **80**, 778 (1998).
- [27] J. Bibette, T. G. Mason, H. Gang, D. A. Weitz, and P. Poulin, *Langmuir* **9**, 3352 (1993).
- [28] P. Poulin, J. Bibette, and D. A. Weitz, *Eur. Phys. J. B* **7**, 277 (1999).